JOURNAL OF PROPULSION AND POWER
Vol. 8, No. 3, May–June 1992

Some Effects of Oscillation Waveform and Amplitude on Unsteady Turbulent Shear Flows

Naval K. Agarwal,* Roger L. Simpson,† and B. G. Shivaprasad‡
Virginia Polytechnic Institute and State University, Blacksburg, Virginia 24061

Some physical features of several unsteady separating turbulent boundary layers are presented for practical Reynolds numbers and reduced frequencies such as for helicopter and turbomachinery flows. The effects of unsteadiness amplitude and waveform are examined for flows along the floor of a converging and diverging wind tunnel test section. At the end of the converging portion, the mean skin friction coefficient normalized on the mean dynamic pressure is independent of the waveform and amplitude within low experimental uncertainties. In the detaching and detached portions of the flow, wall values of the fraction of time that the flow moves downstream $\hat{\gamma}_{pu}$, which is a separated flow state variable, shows that oscillation waveform and amplitude strongly influence the detached flow behavior. Distributions of $\hat{\gamma}_{pu}$ during a cycle indicate hysteresis within the detached flow and the effects of the higher harmonics of pressure gradient and velocity.

Nomenclature

C_p = pressure coefficient, $2(P - P_i)/\rho\bar{U}_{ei}^2$
$\hat{C}_f/2$ = $\hat{\tau}_w/\rho\hat{U}_e^2$, ensemble-averaged skin-friction coefficient
$\bar{C}_{fs}/2$ = $\bar{\tau}_w/\rho\overline{U_e^2}$, mean skin friction coefficient using mean velocity
$\bar{C}_{fu}/2$ = $\bar{\tau}_w/\rho\overline{U_e^2}$, mean skin friction coefficient using mean dynamic pressure
c = length of converging-diverging portion of test section, 4.9 m
f = frequency of flow oscillation, Hz
$\hat{H}$ = $\hat{\delta}^*/\hat{\theta}$, shape factor
$\hat{K}$ = acceleration parameter, $\nu/\hat{U}_e^3[\partial\hat{U}_e/\partial t + \hat{U}_e\partial\hat{U}_e/\partial X]$
k = $\omega c/2\bar{U}_{ei}$, reduced frequency
$\hat{N}$ = distance from the wall to the minimum velocity in the ensemble-averaged velocity profile backflow
p = pressure
R = $(\hat{U}_{ei\ \max} - \hat{U}_{ei\ \min})/2\bar{U}_{ei}$
R_{ne} = $\bar{U}_{ne}/\bar{U}_e$
t = time
$\bar{U}$, $\hat{U}$ = time-averaged velocity, ensemble-averaged velocity
$\bar{U}_{ei}$ = mean test section entrance velocity
$\hat{U}_N$ = maximum backflow velocity
$\bar{U}_{ne}$ = amplitude of nth harmonic
X, Y, Z = streamwise, normal, and spanwise coordinates
γ_{1e} = phase angle of first harmonic of pressure gradient
γ'_{1e} = $\gamma_{1e} + \phi_{1e} + 180$ deg
$\hat{\gamma}_{pu}$ = ensemble-averaged forward flow fraction
$\hat{\delta}^*$ = displacement thickness
$\hat{\theta}$ = momentum thickness
ν = kinematic viscosity
ρ = density
$\overline{\tau_w}$, $\hat{\tau}_e$ = mean and ensemble-average wall shearing stress
ϕ_{1e} = phase angle of first harmonic of velocity
ω = $2\pi f$

Subscripts
e = freestream condition outside shear flow
ei = freestream entrance condition
max, min = maximum and minimum values
n = harmonic number, e.g., 1, 2, etc.

Introduction

EXPERIMENTAL information on unsteady turbulent boundary layers is of practical interest because of unsteady aerodynamic phenomena associated with blades in compressors and turbines, and with helicopter rotors in translating motion. In addition to proper understanding of the physical behavior of these flows, the experimental information is necessary for developing proper calculation methods.

In spite of its importance, relatively little fundamental work has been done to describe the structure of unsteady separating turbulent shear layers. Although nonsinusoidal oscillations are more common in practice, to the authors' knowledge no investigation concerning effects of waveform shape or amplitude on the flow behavior has been reported, particularly for separated flows. Simpson et al.[1,2] and Cousteix et al.[3] were the first to make measurements of the oscillating Reynolds stresses in separating flows. Parikh et al.[4] and Jayaraman et al.[5] examined some cases with small amounts of near-wall reversed flow during parts of a cycle, but with no flow detachment. In all these experiments the maximum value of amplitude to mean freestream velocity ratio was about 0.3.

The purpose of this paper is to present new, previously unpublished, data on a compressor waveform flow ($R = 0.238$) and a large amplitude flow ($R = 0.752$) (Fig. 1) with $k = 0.63$. These results are compared with those from two large amplitude flows ($R_{1e} \simeq 0.75$ and $k = 0.61$ and 1.33) of Agarwal and Simpson.[6–10] These large amplitude flows show some unique features not observed in the compressor waveform flow and moderate amplitude flows, ($R_{1e} = 1/3$) of Simpson et al.[1,2] Important features of these large amplitude flows are reiterated here as background for discussion of the new data.

During strongly decelerating and minimum freestream velocity phases, intermittent backflow occurs near the wall in

Received Oct. 4, 1989; revision received Nov. 2, 1990; accepted for publication May 30, 1991.

*Visiting Assistant Professor, Department of Aerospace and Ocean Engineering; currently Senior Scientist, Analytical Services and Materials, Inc., 107 Research Drive, Hampton, VA 23666. Associate Fellow AIAA.

†Jack E. Cowling Professor, Department of Aerospace and Ocean Engineering. Fellow AIAA.

‡Research Scientist.

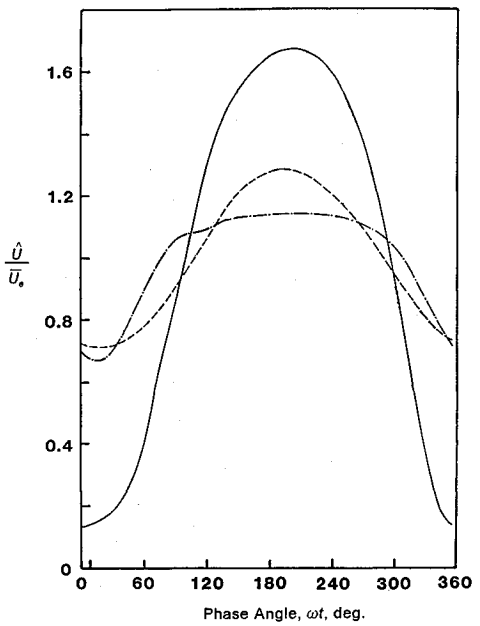

Fig. 1 Unsteady flow waveforms at throat of wind tunnel test section (X = 1.62m). ——large amplitude, R = 0.752, - - - - sinusoidal waveform R = 0.287; -·-·- compressor type waveform, R = 0.238.

the converging section of the tunnel (Fig. 2). Phase ensemble-averaged velocity profiles at these phases in the presence of intermittent backflow are quite different than those compared to high velocity phases. The velocity profiles at the phases when the flow is accelerating, e.g., $0 \leq \omega t \leq 45$ deg in Fig. 1, are very similar to those for strongly accelerated steady flows, whereas at 330 deg $\leq \omega t \leq$ 360 deg when the flow is highly decelerating, velocity profiles are similar to typical high adverse gradient steady flows.[11] In addition, very high values of the acceleration parameter $\hat{K}$ at some accelerating flow phases ($>3.6 \times 10^{-6}$, k = 0.61 flow; $>4 \times 10^{-5}$, k = 1.33 flow) are sufficient to produce laminarescent ensemble-averaged profiles during a short portion of the cycle.[7,8,10]

In this paper detachment is defined as the location where the phase-averaged or ensemble-averaged flow leaves the wall with a zero ensemble-averaged wall shear stress. This location is also where the ensemble-averaged fraction of time that the flow moves downstream, i.e., $\hat{\gamma}_{pu}$ is $\frac{1}{2}$ (see Ref. 11). Simpson[12] observed that if $\hat{\gamma}_{pu} < \frac{1}{2}$ near the wall, along with a low Reynolds shearing stress near the wall, phase-ensembled-averaged backflow $\hat{U}/|\hat{U}_N|$ is a function of $(y/\hat{N})$. Although large phase variations exist through the downstream detached shear flow, Simpson et al.[1,2] and Agarwal and Simpson[10] observed that when $\partial\hat{\gamma}_{pu}/\partial t < 0$, for a given $\hat{\gamma}_{pu}$, $\hat{U}/\hat{U}_e$ vs $y/\hat{\delta}^*$ phase-ensemble-averaged velocity profiles are the same and also agree well with steady-flow profiles at the same $\hat{\gamma}_{pu}$. Therefore, $\hat{\gamma}_{pu}$ can be used as a diagnostic parameter near the wall, which can describe the flow behavior.

For all of the unsteady flows studied,[1,2,6-10] the flow is quasi-steady upstream of detachment at the phases with no flow reversal, and seems to be independent of waveform shape and amplitude. After the beginning of detachment, large amplitude and phase variations develop through the flow and the structure is not quasisteady.

Very large backflow velocities exist in large amplitude flows; some phases of cycle they are even larger than the freestream velocity. While turbulence energy diffusion and dissipation are dominant in low-velocity backflows, during these large backflows significant turbulence energy production and a non-zero Reynolds shearing stress also occur near the wall and $\gamma_{pu} \approx 0$. Agarwal and Simpson[9] have shown that in these large amplitude flows with substantial turbulence energy production near the wall, a normal turbulent boundary layer type behavior occurs in the backflow region. This behavior is significantly different than that for the moderate amplitude flows, (R_{1e} = 1/3) where moderate backflow velocities ($\hat{U}_N/\hat{U}_e \sim$ 0.3) and negligible Reynolds shearing stress and turbulence energy production occur near the wall. Simpson's[12] mean backflow correlation does not hold in the backflow region for large backflows. Large and negative values of the phase ensemble-averaged velocity profile shape factor $\hat{H}$ and hysteresis between flow parameters were observed. The hysteresis and $\hat{H}$ both increase with reduced frequency and flow oscillation amplitude.

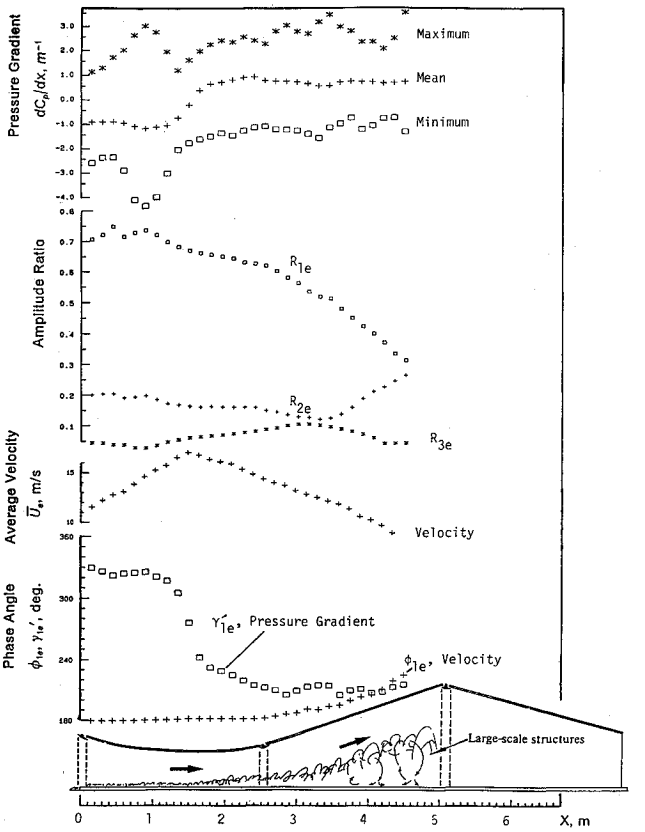

Fig. 2 Phase angle of first harmonic, ϕ_{1e}, γ'_{1e}; freestream velocity $\hat{U}_e$, amplitude to mean velocity ratio and pressure distributions along the tunnel centerline for the large amplitude flow, k = 1.33.

Practical flows in compressors and turbines may have non-sinusoidal waveforms and, therefore, it is important to know the effects of waveform and amplitude of oscillation on the flow behavior. In turbomachinery, the unsteadiness is a result of the periodic wakes produced by the rotor vanes as they move past the stator and vice versa. The waveform shape is dependent on the various geometrical and operating conditions of the machine. Experimentally, it is difficult to simulate exactly any particular waveform shape. Although the waveform may consist principally of a given frequency, substantial contributions normally come from higher harmonics. Results for some representative waveform shapes with some higher harmonic contents are presented here.

Description of Test Flows

Simpson et al.[1,2] presented experimental measurements in two moderate amplitude sinusoidal waveform unsteady flows ($R_{1e} \sim$ 1/3) at reduced frequencies, k of 0.61 and 0.90. Agarwal and Simpson[6-10] presented experimental measurements in two large amplitude flows with k = 0.61 and 1.33, $\tilde{U}_{ei}$ = 15.04 m/s and 11.06 m/s, and R = 0.63 and 0.74, respectively. These measurements are compared with a compressor type waveform flow and another large amplitude flow ($R \sim$ 0.75 with k = 0.63, and $\hat{U}_{ei}$ = 14.71 m/s), which are presented here. The frequency of flow oscillations in the k = 0.63 and 0.61 flows was the same, 0.596 Hz, whereas for the k = 1.33 flow, it was 0.954 Hz.

The same wind tunnel test section (Fig. 2) was used in these experiments at Southern Methodist University and VPI&SU. Unsteadiness was produced by an instream rotating-blade damper system, described by Simpson, et al.[13] In this system the angular velocity of the rotating blades is varied during a cycle in order to produce the described waveform, amplitude, and frequency of the flow entering the test section. All of the events during an oscillation cycle were synchronized with respect to a "reference" square wave voltage signal at the oscillation frequency generated by the quartz clock in the control electronics. The experimental facility with active boundary-layer control on nontest top and side walls (Fig. 2) and the hot-wire and laser anemometers used in these measurements have been previously described in detail by Simpson et al.[1,2] and Agarwal and Simpson.[8,10] Detailed velocity and turbulence measurements for the large amplitude flows ($k = 0.63$ and 1.33) are reported in Refs. 6, 7, 8, and 10. Various waveforms used in the experiments are shown in Fig. 1.

The phase ensemble-averaged freestream velocity $\hat{U}_e$ outside the boundary layer can be expressed in terms of its Fourier components $\hat{U}_{ne}$ as

$$\hat{U}_e = \overline{U_e}\left\{1 + \sum_{n=1}^{\infty}\left[\frac{\hat{U}_{ne}}{\overline{U_e}}\cos(\omega nt - \phi_{ne})\right]\right\} \quad (1)$$

Using the streamwise velocity distributions, the freestream streamwise pressure gradient was calculated from the unsteady Bernoulli equation. Phase-ensemble-averaged quantities were obtained by ensemble-averaging the measurements for that phase over at least 200 cycles. Here we denote phase-ensemble-averaged quantities by a caret above the symbol. Figure 2 shows the mean freestream velocity and amplitude of higher harmonics for a large amplitude flow ($k = 1.33$). Although the rotating damper tends to smooth out the higher harmonics, they appear to be important for the large amplitude flows. Nondimensional mean, maximum, and minimum pressure gradients dC_p/dx along the centerline of the test wall and the phase angles of the first harmonics of the freestream velocity ϕ_{1e} and the pressure gradient γ'_{1e} are also shown in Fig. 2. (It should be noted that the ϕ_{1e} for the $k = 0.63$ large amplitude and compressor waveform flows is shown 40 deg higher because $\omega t = 0$ was taken at a different phase.) The first harmonic pressure gradient strongly lags the local freestream velocity in the converging section of the tunnel upstream of 2 m in all the large amplitude flows studied. The lag is considerably lower in the diverging section and after detachment the first harmonic of the oscillating pressure gradient only slightly lags or equals the first harmonic of the velocity oscillations.

Mean Skin-Friction Coefficients

Measurements of the skin friction were made using a Rubesin et al.[14]-type surface hotwire gage described by Simpson et al.[11] Because the outer region of accelerating turbulent boundary layers does not have a strong wake component and is largely governed by wall conditions, the waveform and amplitude effects on the skin friction were examined at the throat or minimum flow area (1.62 m) of the wind tunnel, just downstream of the converging section where the flow was accelerating most of the time.

Two series of experiments were conducted. In the first, the waveform shape was varied with a nearly constant R, and in the second case the R was varied with a nearly same freestream velocity distribution. The $\bar{C}_{fs}$ skin friction coefficient is defined as

$$\frac{\bar{C}_{fs}}{2} = \frac{\bar{\tau}_w}{\rho\overline{U_e^2}} \quad (2)$$

As shown in Table 1 for the cases with nearly constant R, $\bar{C}_{fs}$ varied about 10% for the different waveforms, three of which are shown in Fig. 1. In each case, the mean freestream velocity $\bar{U}_e$ of 21.45 m/s was the same at the test-section throat. Note that the $\bar{U}_e$ in these experiments is the same as the steady flow experiments of Simpson et al.[11] using the same facility.

Table 1 Effect of waveform shape on mean skin-friction coefficient

R	$\left(1 + \frac{1}{2}\sum_{n=1}^{5} R_{ne}^2\right)$	$\frac{\bar{C}_{fs}}{2} \times 10^3$	$\frac{\bar{C}_{fu}}{2} \times 10^3$
0.287	1.042	1.61	1.55
0.263	1.036	1.59	1.54
0.284	1.039	1.74	1.68
0.269	1.036	1.74	1.68
0.238	1.025	1.73	1.69
0.247	1.031	1.74	1.69

Table 2 Effect of amplitude-ratio on mean skin-friction coefficient

R	$\left(1 + \frac{1}{2}\sum_{n=1}^{5} R_{ne}^2\right)$	$\frac{\bar{C}_{fs}}{2} \times 10^3$	$\frac{\bar{C}_{fu}}{2} \times 10^3$
0.287	1.042	1.61	1.55
0.295	1.046	1.58	1.51
0.534	1.146	1.75	1.53
0.752	1.306	2.07	1.59

Squaring both sides of Eq. (1) and time averaging leads to the relation

$$\overline{U_e^2} = \overline{U_e^2}\left[1 + \frac{1}{2}\sum_{1}^{n=5} R_{ne}^2\right] \quad (3)$$

for the first five harmonics of nonsinusoidal waveforms. Higher harmonics are negligible here. A friction factor can be defined that reflects the oscillation contribution to the mean freestream dynamic pressure in Eq. (3):

$$\frac{\bar{C}_{fu}}{2} = \frac{\bar{\tau}_w}{\rho\overline{U_e^2}} \quad (4)$$

Combining Eqs. (2–4) leads to

$$\frac{\bar{C}_{fu}}{2} = \frac{\bar{C}_{fs}}{2\left[1 + \frac{1}{2}\sum_{1}^{n=5} R_{ne}^2\right]} \quad (5)$$

Table 1 also gives the values of $\bar{C}_{fu}$ and R obtained from the phase-averaged values of the freestream velocity. It is clear from Table 1 that $\bar{C}_{fu}/2$ for all the six different waveform cases agree with one another within the limits of experimental uncertainty on $\bar{\tau}_w$, which is ±12%. Furthermore, $\bar{C}_{fu}/2$ for all the six cases agree with the value obtained at that location for steady flow, 0.00168 (Simpson et al.[15]).

Table 2 gives the results of the second series of experiments, i.e., various amplitudes R with the same freestream velocity distribution.

For the highest amplitude studied, ($R = 0.752$), the value of $\bar{C}_{fs}$ for the unsteady flow is much higher and cannot be attributed to experimental uncertainty. Although the high amplitude unsteady flow might have some effect on the mean skin friction coefficient, $\bar{C}_{fu}$ for these cases are within ±2.7% (Table 2). This indicates that the amplitude effect can be accounted for by the oscillation contribution to $\overline{U_e^2}$ in Eq. (4) for $\bar{C}_{fu}$. Hence, from this limited amount of data it can be concluded that both waveform shape and amplitude have little effect on the mean skin friction coefficient $\bar{C}_{fu}$ for attached and accelerating flows.

Downstream-Upstream Flow Intermittency $\hat{\gamma}_{pu}$

Although $\hat{C}_f$ can be used as a parameter for location of separation, its measurement in the near separation zone is

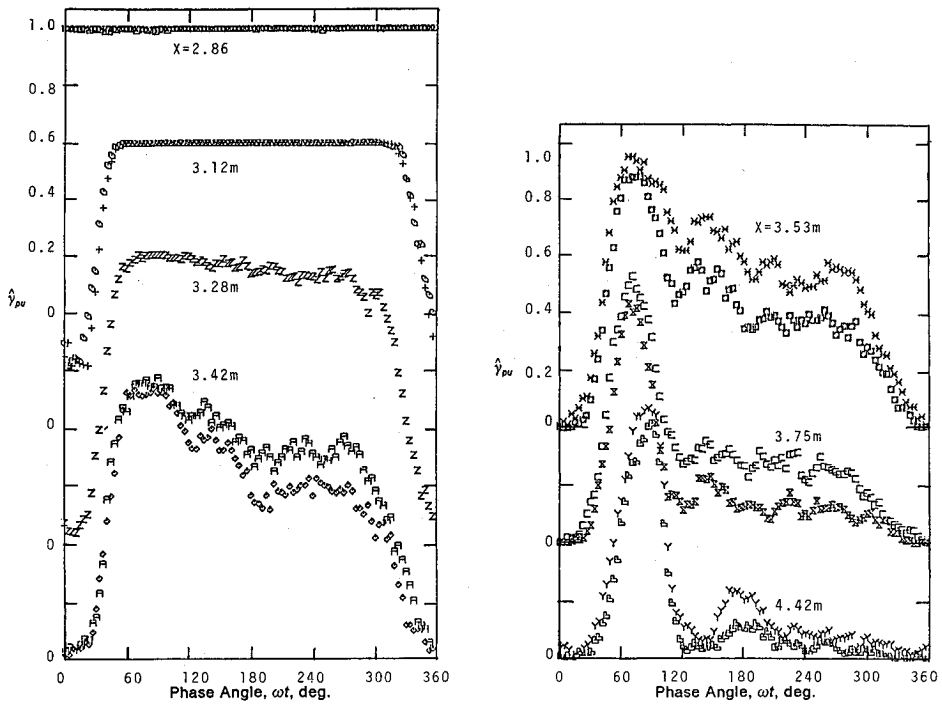

Fig. 3a Phase ensemble-averaged $\hat{\gamma}_{pu}$ from thermal tuft measurements for the compressor waveform flow, $R = 0.238$, $k = 0.63$.

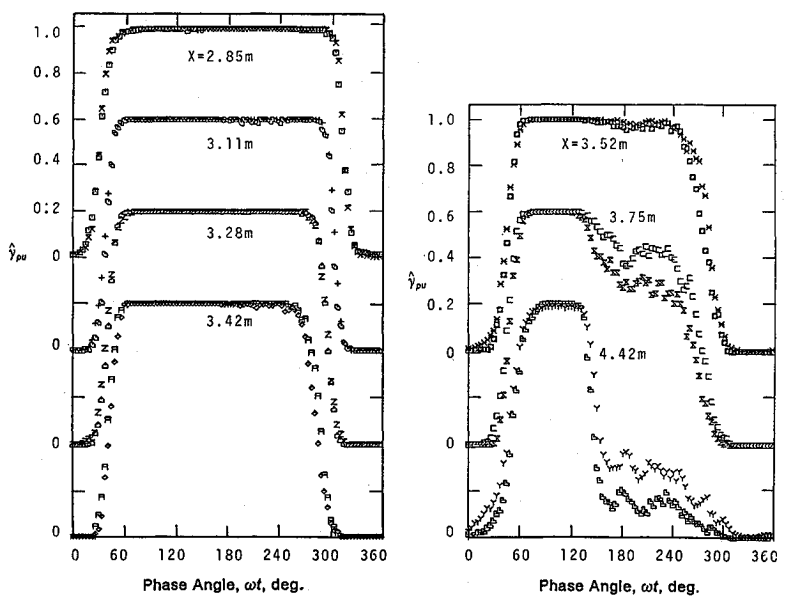

Fig. 3b Phase ensemble-averaged $\hat{\gamma}_{pu}$ from thermal tuft measurements for the large amplitude flow, $k = 0.63$.

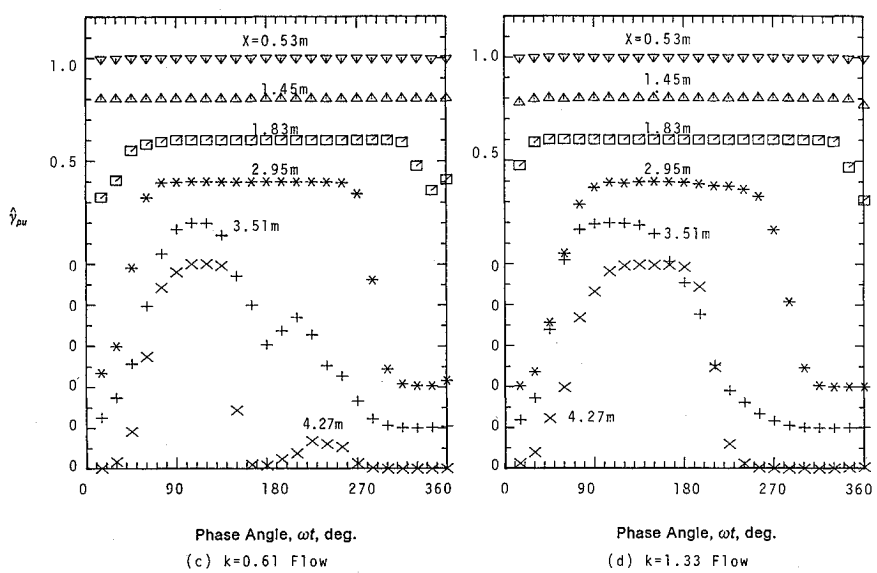

Figs. 3c–3d Phase-ensemble averaged $\hat{\gamma}_{pu}$ from laser anemometer measurements for the large amplitude, $k = 0.61$ and 1.33 flows.

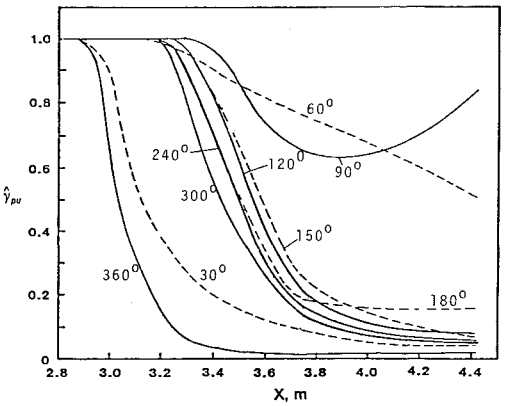

Fig. 4a Phase-ensemble averaged $\hat{\gamma}_{pu}$ vs X for different ωt phases of a cycle for the compressor-type waveform flow, $R = 0.238$, $k = 0.63$.

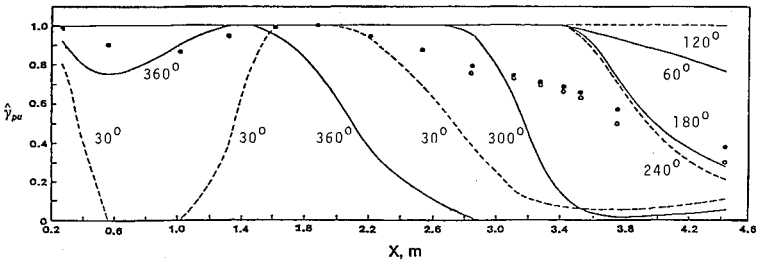

Fig. 4b Phase-ensemble averaged $\hat{\gamma}_{pu}$ vs X for different ωt phases of a cycle for the large amplitude flow, $R = 0.752$, $k = 0.63$.

relatively uncertain because $\hat{C}_f$ approaches zero. A more descriptive parameter is the near wall minimum ensemble-averaged fraction of time the flow moves downstream $\hat{\gamma}_{pu}$ at a given streamwise location, which Simpson et al.[1,2,11,15] used as a diagnostic variable to define the flow behavior in two-dimensional separating turbulent boundary layers. Simpson[16] proposed a set of quantitative definitions as the detachment state near the wall using $\hat{\gamma}_{pu}$: *incipient detachment* (ID) occurs with instantaneous backflow 1% of the time ($\hat{\gamma}_{pu} = 0.99$); *intermittent transitory detachment* (ITD) occurs with instantaneous backflow 20% of the time ($\hat{\gamma}_{pu} = 0.8$); *transistory detachment* (TD) occurs with instantaneous backflow 50% of the time ($\hat{\gamma}_{pu} = 0.5$); and *detachment* occurs where the time-averaged wall shear stress $\bar{\tau}_w$ is zero. Results of Simpson et al. indicate that TD and D occur at the same location.

Near wall minimum values of γ_{pu} occur 1 mm from the test wall in the steady freestream flow examined in this facility. Consequently, $\hat{\gamma}_{pu}$ was measured at 1 mm from the test wall using a laser anemometer in the large amplitude $k = 0.61$ and 1.33 flows and by using a heated wake direction-sensing thermal tuft, similar to one used by Eaton et al.[17] and described by Shivaprasad and Simpson,[18] in the $k = 0.63$ large amplitude and compressor waveform flows. The results from the thermal tuft were obtained for the two possible probe orientations 180 deg apart and are at most ± 0.1 uncertain, although at most phases agreement is better than this. Note that the $k = 0.63$ and $k = 0.61$ large amplitude flows are nearly the same and were measured several years apart using different techniques.

Some of the important results for the moderate amplitude flows are reiterated here (see Refs. 1 and 2 for more details). As the freestream velocity during a cycle begins to increase, the fraction of time that the flow moves downstream $\hat{\gamma}_{pu}$ at a given phase of the cycle increases as backflow fluid is washed downstream.[1,2] (Refer to Fig. 18 of Simpson et al.[1] and Fig. 8 of Simpson et al.[2]) As the freestream velocity nears the maximum value in a cycle, the increasingly adverse pressure gradient causes progressively greater near wall backflow at downstream locations while $\hat{\gamma}_{pu}$ remains high at the upstream part of the detached flow. For these flows $\hat{\gamma}_{pu}$ never reaches zero, indicating that there is no location with backflow all of the time.

Figures 3a–3d show $\hat{\gamma}_{pu}$ vs ωt for the axial-compressor-type waveform and large amplitude flows. For the compressor-type-waveform (Fig. 3a), as in the moderate amplitude flows, the backflow is washed downstream and the detached shear layer thickness decreases as the freestream flow accelerates during 20 deg $< \omega t <$ 60 deg. Similar effects are evident for large amplitude flows in Figs. 3b–3d. For 60 deg $< \omega t <$ 90 deg, $\hat{U}_e$ continues to increase and $\hat{\gamma}_{pu}$ remains high for all the cases. For $\omega t >$ 90 deg the cessation of the unsteady acceleration (refer to Fig. 1) causes an adverse pressure gradient, which results in a sudden decrease in $\hat{\gamma}_{pu}$, particularly in the downstream detached flow region. For the compressor-type waveform case for 120 deg $< \omega t <$ 300 deg, $\hat{U}_e$ is nearly constant and the observed small variation of $\hat{\gamma}_{pu}$ with ωt is principally due to second and higher harmonic effects. As $\hat{U}_e$ decreases for $\omega t <$ 300 deg, $\hat{\gamma}_{pu}$ decreases. These second and higher harmonic effects are evident for all the cases except the large amplitude flow with $k = 1.33$.

Figures 4a–4d show $\hat{\gamma}_{pu}$ vs X at various ωt for these flows. It is clear from these figures (and also for the moderate am-

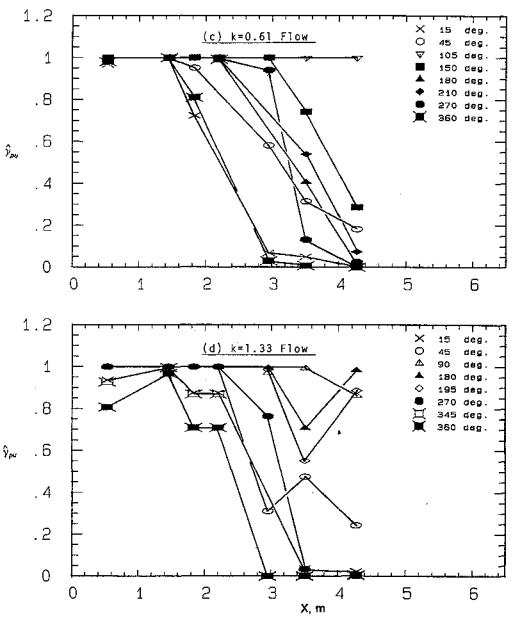

Figs. 4c–4d Phase-ensemble averaged $\hat{\gamma}_{pu}$ vs X for different ωt phases of a cycle for the large amplitude, $k = 0.61$ and 1.33 flows

plitude flows[1,2]) that at some phases of the cycle, the backflow is completely washed out with $\hat{\gamma}_{pu}$ becoming unity. Similar effects were observed by Simpson et al.[1,2] for their moderate amplitude flows. As the freestream velocity reaches the maximum velocity, $\hat{\gamma}_{pu}$ decreases in the downstream zone. At larger ωt, $\hat{\gamma}_{pu}$ drops to very low values in the downstream zone and is zero at some phases of the oscillation cycle, indicating that there is backflow all the time.

For the case of large amplitude flows, at low velocity phases close to the wall intermittent backflow occurs upstream of the tunnel throat (minimum cross-sectional area location) (Figs. 3c, 3d, 4c, 4d). This is a significant difference compared to the moderate amplitude flows of Simpson et al.[1,2] and the compressor waveform flow.

Discussion

In all the flows presented here, flow separation was caused by an increasingly adverse pressure gradient in the diverging portion of the test section. The pressure gradient calculations using the unsteady inviscid equation of motion involves R_{ne}^2 terms, whereas the velocity distribution in Eq. (1) has only R_{ne} terms. Therefore, the pressure gradient is more affected by the higher harmonics than the velocity distributions. Results of Agarwal and Simpson[6,8,10] show that in large amplitude flows, higher harmonics of the pressure gradient are produced that subject the boundary layer to several pressure gradient oscillations per cycle of the velocity. Figures 3a–3c show that the near-wall downstream-upstream intermittency $\hat{\gamma}_{pu}$ seems to be strongly affected by freestream pressure gradient oscillations. The effects of second and higher harmonics are evident in Figs. 3a–3c for the compressor waveform flow and the $k = 0.63$ and $k = 0.61$ large amplitude flows, but not in the $k = 1.33$ (Fig. 3d) large amplitude flow. These effects were not observed in a low amplitude flow ($R_{1e} = 0.12$ and $R = 0.17$ with $k = 1.03$) study by Agarwal and Simpson.[19] It should be noted that the frequency of flow oscillations in both of these latter cases was 0.954 Hz. Therefore, the absence of higher harmonic effects can be explained that at higher frequencies of flow oscillation the near wall flow has little time to respond to higher harmonic pressure gradient oscillations. Figures 3a–3d clearly show the hysteresis in flow after the detachment.

Conclusions

Upstream of separation, the ensemble-averaged characteristics of the flow are unaffected by flow oscillations or amplitude at the phases with no instantaneous flow reversal.

Neither waveform shape nor amplitude seem to affect the skin friction coefficient $\bar{C}_{fu}$ for attached accelerating unsteady turbulent boundary layers. For all the cases considered, the average $\bar{C}_{fu}/2$ agreed with the steady flow value because the mean dynamic pressure was made to account for the different harmonics present in the flow.

Earlier measurements[1,2,10] of $\hat{\gamma}_{pu}$ have shown that $\hat{\gamma}_{pu}$ can be used as a diagnostic parameter for the detachment state of steady and unsteady turbulent shear flows and $\hat{\gamma}_{pu}$ measurements indicate considerable effects of waveform shape and amplitude downstream of detachment. Both the compressor waveform and large amplitude flows with $k = 0.61$ and 0.63 indicate dips in the $\hat{\gamma}_{pu}$ vs ωt distributions with later secondary peaks, which can be attributed to higher harmonic effects. Therefore, downstream of detachment, waveform shape and amplitude strongly affect the flow behavior. This is an important conclusion because nonsinusoidal waveform flows exist in turbomachinery.

Acknowledgments

This work was supported by NASA Ames Grant NSG-2354 monitored by J. Marvin and Air Force Office of Scientific Research Grant 84-0134 monitored by J. McMichael and H. Helin.

References

[1]Simpson, R. L., Shivaprasad, B. G., and Chew, Y.-T., "The Structure of a Separating Turbulent Boundary: Part 4, Effects of Periodic Free-Stream Unsteadiness," *Journal of Fluid Mechanics,* Vol. 127, 1983, pp. 219–261.

[2]Simpson, R. L., and Shivaprasad, B. G.,"The Structure of a Separating Turbulent Boundary Layer: Part 5, Frequency Effects on Periodic Unsteady Freestream Flows," *Journal of Fluid Mechanics,* Vol. 131, 1983, pp. 319–339.

[3]Cousteix, J., Houdeville, R., and Raynaud, M., "Oscillating Turbulent Boundary Layer of an Unsteady Turbulent Boundary Layer," NASA TR. TH75799-N8017400.

[4]Parikh, P. G., Reynolds, W. C., Jayaraman, R. and Carr, L. W., "Dynamic Behavior of an Unsteady Turbulent Boundary Layer," *Unsteady Turbulent Shear Flows,* edited by R. Michel, Springer-Verlag, New York, 1987, pp. 35–36.

[5]Jayaraman, R., Parikh, P., and Reynolds, W. C., "An Experimental Study of the Dynamics of an Unsteady Turbulent Boundary Layer," Thermosciences Div., Dept. Mech. Engrg., Stanford Univ. TR TF-18, Stanford, CA, 1982.

[6]Agarwal, N. K., and Simpson, R. L., "The Structure of Large Amplitude Unsteady Separating Turbulent Boundary Layers," AIAA Paper 87-0191, Twenty-fifth Aerospace Sciences Meeting, Jan. 12–15, 1987, Reno, NV.

[7]Agarwal, N. K., and Simpson, R. L., "Experimental Measurements of the Structure of a Large Amplitude Unsteady Separating Turbulent Boundary Layers," *Proceedings of Air Force Office of Scientific Research Workshop II on Unsteady Separated Flows,* Sept. 1988, pp. 147–153.

[8]Agarwal, N. K., and Simpson, R. L., "Experimental Study of Unsteady Separating Turbulent Boundary Layers," Final TR AFOSR-88-0271TR, Aerospace and Ocean Engrg., VPI&SU, Blacksburg, VA, Feb. 1988; also AD-A192997.

[9]Agarwal, N. K., and Simpson, R. L., "The Structure of Backflow Profiles in Unsteady and Steady Separating Turbulent Boundary Layers," *AIAA Journal,* Volume 10, No. 10, 1990, pp. 1766–1771; also AIAA Paper 89-0567.

[10]Agarwal, N. K., and Simpson, R. L., "Separating Turbulent Boundary Layers with Very Large Ampiltude Unsteadiness," *Journal of Fluid Mechanics* (submitted for publication).

[11]Simpson, R. L., Shivaprasad, B. G., and Chew, Y.-T., "The Structure of a Separating Turbulent Boundary Layer: Part 1, Mean Flow and Reynolds Stresses," *Journal of Fluid Mechanics,* Vol. 113, 1981, pp. 23–74.

[12]Simpson, R. L., "A Model for the Backflow Mean Velocity Profile," *AIAA Journal,* Vol. 21, 1983, pp. 142–143.

[13]Simpson, R. L., Sallas, J. J., and Nasburg, R. E., "Tailoring the Waveform of a Periodic Flow with a Programmable Damper," *Journal of Fluids Engineering,* Vol. 100, 1978, pp. 287–290.

[14]Rubesin, M. ., Okumo, A. F., Mateer, G. G., and Brosh, A., "A Hot-Wire Surface Gage for Skin-Friction and Separation Detection Measurements," NASA, TM X-62, 1975, 465.

[15]Simpson, R. L., Chew, Y.-T., and Shivaprasad, B. G., "The Structure of a Separating Turbulent Boundary Layer: Part 2, Higher Order Turbulence Results," *Journal of Fluid Mechanics,* Vol. 113, 1981, pp. 53–73.

[16]Simpson, R. L., "Two Dimensional Turbulent Separated Flow," AGARDograph 287, 1985.

[17]Eaton, J. K., Jeans, A. H., Ashjaee, J., and Johnston, J. P., "A Wall Flow-Direction Probe for Use in Separating and Reattaching Flows," *Journal of Fluids Engineering,* Vol. 101, pp. 364–366.

[18]Shivaprasad, B. G., and Simpson, R. L., "Evaluation of an Improved Wall-Flow-Direction Probe for Measurements in Separated Flows," *Journal of Fluids Engineering,* Trans. of American Society of Mechanical Engineers, Vol. 104, 1982, pp. 162–166.

[19]Agarwal, N. K., and Simpson, R. L., "A Separating Turbulent Boundary Layer with an Unsteady Diverging Free-Stream," *Experiments in Fluids* (submitted for publication).